

AD-A142 183

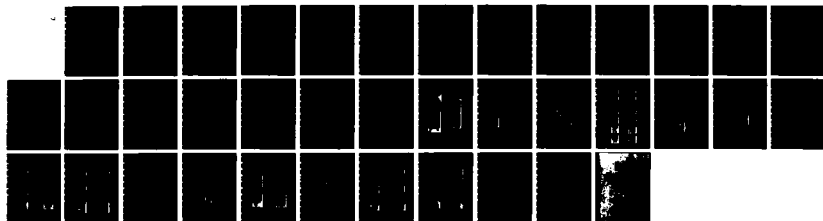
PLASMA STUDIES ON ION DIODES(U) MASSACHUSETTS INST OF  
TECH CAMBRIDGE RESEARCH LAB OF ELECTRONICS G BEKEFI  
05 APR 83 N00014-82-K-2036

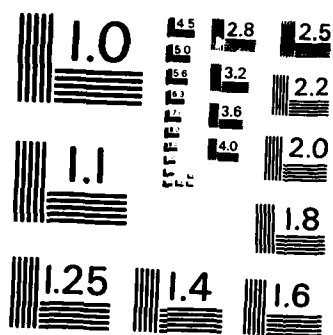
1/1

UNCLASSIFIED

F/G 20/9

NL





MICROCOPY RESOLUTION TEST CHART  
NATIONAL BUREAU OF STANDARDS - 1963 - A

AD-A142 183

FINAL REPORT

Plasma Studies on Ion Diodes

Office of Naval Research  
Contract N00014-82-K-2036

covering the period  
15 December 1981 - 15 December 1982

Submitted by  
G. Bekefi

5 April 1983

DTIC  
SEL  
JUN 10 1984  
A

MASSACHUSETTS INSTITUTE OF TECHNOLOGY  
Research Laboratory of Electronics  
Cambridge, Massachusetts 02139

This document has been approved  
for public release and sale; its  
contents are not classified.

84 06 15 055

DTIC FILE COPY

MASSACHUSETTS INSTITUTE OF TECHNOLOGY  
RESEARCH LABORATORY OF ELECTRONICS  
CAMBRIDGE MASS 02139

Final Scientific Report on ONR Contract N00014-82-K-2036

for research on

Plasma Studies on Ion Diodes

for the period

December 15, 1981 - December 15, 1982

PROJECT SUMMARY

✓  
Cathode plasmas in pulsed high current vacuum diodes have been studied using optical interferometry and spectroscopy. Both aluminum and graphite cathodes were used and the diode current density was varied over a factor of ten. The cathode plasma inventory was seen to increase during the length of the pulse and the plasma density was seen to increase with increasing current density. Spectral line emission from H, CI, CII, and CIII was observed when either cathode was used. It is concluded that cathode plasma expansion is dominated by protons from cathode surface contaminants.

↖



### Introduction

The properties of the plasma layer formed on the cathodes of pulsed vacuum diodes and magnetically insulated transmission lines (MITL's) determine many aspects of the behavior of these devices. For example, electron flow may be affected by plasma instabilities whose growth rates depend on the plasma parameters,<sup>1,2</sup> and the pulse length is often limited by gap closure due to expansion of the cathode and anode plasmas. To control these effects, then, it becomes necessary to control the composition, density, and/or temperature of the cathode plasma.

A relevant question concerns the importance of surface contaminants such as the thin layers of pump oils which will exist in most practical vacuum systems. If these impurities dominate cathode plasma formation then variations in cathode material and surface preparation will have little effect on the cathode plasma properties.

It is worth noting that the processes of energy supply to the cathode may vary widely from device to device. The density of current drawn from the cathode into the cathode plasma, for example, may range from several hundred kA/cm<sup>2</sup> in an intense ion beam diode to less than 1kA/cm<sup>2</sup> in a long MITL. Qualitative variations are also to be expected, ranging from localized resistive heating of cathode protrusions to a broad area, short range deposition of energy, due to electron bombardment in a MITL<sup>3</sup> or soft x-ray fluences from a nearby load.<sup>4</sup> The cathode plasma properties, as well as the relative importance of surface contaminants in determining these properties, may thus be expected to depend on the particular diode.

The objectives of the work reported here were to determine the importance of surface impurities in cathode plasma formation in a specific diode, and then to investigate the relevance of these results to other experiments by varying the current density drawn from the cathode over a factor of ten. This is a continuation of work reported earlier.<sup>5</sup>

### Experiment

This experiment involves spectroscopic and interferometric studies of cathode plasmas in a planar diode. The importance of surface contaminants was inferred by noting the effect of a variation in cathode material and surface preparation on the cathode plasma parameters, and the current density was varied over a factor of ten by varying the cathode area. The diode was driven by a Sandia Nereus accelerator, with peak voltages and currents of about 240kV and 60kA, respectively, and 80 nsec pulse lengths.

Typical cathodes are shown in Fig. 1. They are in the form of bars with lengths of 7cm and widths ranging from 3mm to 25mm, yielding peak current densities which ranged from about 27kA/cm<sup>2</sup> to 3 kA/cm<sup>2</sup>, respectively. The cathodes, which were replaced after every shot, were machined from 2024 aluminum. Various types of surface finish were used and for some of the shots the cathodes were coated with a spray-on graphite coating (Aerodag G)<sup>6</sup>. In this case, the coating was thick enough to completely cover the aluminum -- no aluminum spectral lines were observed, nor was any aluminum visible under the graphite after the shot. The cathodes were cleaned with NaOH, followed by HNO<sub>3</sub>, followed by ultrasound before each shot (and before coating with graphite) to remove any foreign material prior to pumpdown.

The diode vacuum was typical for high current accelerators with a (diffusion pumped) pressure of about  $3 \times 10^{-4}$  T and no cold trap. Standard silicone diffusion pump and hydrocarbon roughing pump oils were used.

A schematic of the experimental arrangement is shown in Fig. 2. Power was fed to the diode by a single-sided vacuum feed -- the gap in the feed region was set large enough to confine plasma formation to the diode. The anodes consisted of slabs of reactor grade graphite which were baked out to remove any machining oils and then allowed to equilibrate with the ambient air. The anode-cathode gaps ranged from 2.1 to 3.5mm, depending on the cathode surface area.

A Mach-Zehnder interferometer with a double pulse nitrogen laser ( $3371\text{\AA}$ ) was used to diagnose the plasma density. The length of each pulse was less than 2ns and the interpulse spacing could be varied. The two laser beams were aligned to pass, almost collinearly, along the 7cm dimension of the cathode surface. The spatial resolution in the direction across the A-K gap was about 0.1 mm; the spatial resolution in the direction along the cathode width was limited by the finite crossing angle between the two beams to about 0.3mm.

As shown in Fig. 2, some of the light from the cathode plasma passed through slots in the anode structure and was imaged onto the entrance slits of three spectrometers. The 0.5M spectrograph had its slit imaged across the A-K gap and was used with photographic film to record time integrated spectral lines. The 0.3M and 0.1M monochromators had their slits imaged parallel to, and about 0.5mm from, the cathode surface. They were used with photomultiplier

tubes to obtain time resolved information on line intensities.

The interferograms yield line averaged densities; in order for these measurements to be of any use, then, it is necessary that the plasma be fairly uniform (in a macroscopic sense) along the line of sight. This could not be observed directly, but was inferred from observations of current flow: x-ray pinhole photographs of the anode (indicative of early time, high voltage electrons) and visual analysis of the anode damage patterns (indicative of later time, lower voltage electrons). Four surfaces are listed in order of decreasing inferred uniformity of current flow in Table 1. In general, the best results were obtained with aluminum cathodes which had been sandblasted with 50 grit aluminum oxide. When graphite coated cathodes were used, there was a noticeable difference in damage uniformity between cathodes that were sandblasted and those that were left smooth prior to coating with graphite. Unblasted aluminum gave the least uniform damage. As would be expected, the damage uniformity was seen to increase with an increasing rate of rise of the diode voltage pulse. A typical x-ray pinhole photograph and anode damage pattern for a sandblasted aluminum cathode are shown in Fig. 3, showing the relative (inferred) emission uniformity.

Electrons impinging on the anode will (given enough time) turn on an anode plasma and energy deposition in the cathode by the resulting ion current will make interpretation of the observed cathode plasma properties more complicated. Analysis of anode damage patterns from shots where the diode was prematurely crowbarred, however, indicates that ion flow does not occur until near the end of the pulse. For the first seventy or so ns of the pulse, then,



anode effects will be neglected. Direct measurements of the ion current with Faraday cups are planned for the future.

### Results

Current and inductively corrected voltage waveforms are shown in Fig. 4a. A 6mm wide graphite coated cathode was used for this particular shot, but these waveforms were typical of all shots. The double hump in the current trace is due to the properties of the Nereus accelerator. The bars on the current trace indicate the times when the interferograms in Fig. 4b were taken. Reference interferograms, which were taken immediately before each shot, are shown on the left. The deviation of the fringes from the straight reference fringes is proportional to the local (line averaged) density. Plasma electrons will shift the fringes down while neutrals will shift the fringes up. For the 7cm path length in this experiment, a shift of one fringe corresponds to a plasma electron density of about  $10^{17} \text{cm}^{-3}$ . The area viewed by the interferometer is shaded in Fig. 4c. After about 40ns the plasma density has become great enough to be observed and as time goes on, the observable front expands toward the anode while the density at any fixed point increases. It should be note that the plasma density necessary to close the gap, given by

$$n_e = j / e v_{th}$$

was about  $10^{15} \text{cm}^{-3}$  for the  $14 \text{kA/cm}^2$  current density here, assuming an electron temperature of a few eV; thus, the exact plasma front could not be observed. Note that by the end of the shot the direction of fringe shift is seen to reverse near the cathode. This is seen more clearly in the interferogram in Fig. 5, which was taken at the end of a shot where a 6mm wide graphite

coated cathode was used. Since the timescale is probably too short for recombination,<sup>7</sup> this could be due to a continued boil off of neutrals from the still-hot cathode surface. To interpret neutral induced fringe shifts correctly, it is necessary to know the composition of the neutral matter. For carbon, a neutral density of about  $10^{18}\text{cm}^{-3}$  is required for one fringe shift; for hydrogen the required density is about  $2.5 \times 10^{18}\text{cm}^{-3}$ .<sup>8</sup> So, the neutral density may be estimated at  $\geq 10^{18}\text{cm}^{-3}$ . These observations would tend to imply that most of the material removed from the cathode comes off in the form of neutrals after the pulse, and hence plasma density measurements given here may not be relevant to studies of cathode erosion.<sup>9</sup> Of course, the effect of neutrals on the fringe shift earlier in time cannot be entirely discounted, but spectroscopic observations suggest that the ratio of neutrals to ions is not large enough during the earlier part of the pulse for this to be the case.

The observed plasma density was seen to be dependent on the current density drawn from the cathode. Current traces for shots involving 6mm and 3mm wide graphite coated cathodes are shown in Fig. 6a, with the corresponding interferograms shown in Fig. 6b. The current densities drawn from these cathodes were about 14 and 27kA/cm<sup>2</sup>, respectively. (At a given point in space and time) the plasma density is greater for the higher current density cathode. For comparison, interferograms for a 25mm wide cathode, which had a current density of about 3kA/cm<sup>2</sup>, are shown in Fig. 6c. No plasma is visible in the first interferogram, indicating an electron density of less than about  $2 \times 10^{16}\text{cm}^{-3}$ , while neutrals are seen coming off the cathode in the second. There is not enough

data at present to determine a precise functional relationship between current density and plasma density, however, the data is consistent with a plasma density (at a given point and time) that is proportional to the time integrated current density:

$$n_e \propto \int j dt .$$

In many of these interferograms the plasma density is seen to vary across the cathode surface, being highest at the top edge and decreasing to a minimum at the bottom edge. The reason for this is not known at present, however, to the extent that the cathode plasma density is related to the density of current drawn out of the cathode surface, this density variation could be due to a corresponding variation in current density. That variation, in turn, could be caused by asymmetrical field enhancement at the cathode edges or by asymmetrical accumulation of space charge in the cathode-anode gap, both being related to the single sided nature of the vacuum feed. Another possibility involves incomplete magnetic diffusion into the cathode plasma<sup>0</sup>-- if the skin depth is such that some of the current is forced to flow through the plasma as shown in Fig. 7, then the current density drawn from the cathode will again be higher at the top. Estimates of the skin depth (using Spitzer resistivity, which is reasonable here since the electron thermal velocity exceeds the drift velocity) imply that it is on the order of the plasma thickness.

The plasma density is seen to increase with time; this could be due to a continual plasma resupply or just the expansion of plasma from a dense layer near the cathode. In order to separate these effects, the diode was crowbarred by causing the insulator stack to flash over prematurely. The current traces and interfero-

grams are shown in Fig. 8. The fact that the fringe shifts are seen for the full pulse while none are seen for the crowbarred pulse indicates that current flow after the crowbar point is responsible for an increased plasma density and thus the plasma inventory actually increases with time while current is flowing in the diode.

In Fig. 9, current traces and interferograms are shown for two cathode materials. The interferograms on the left were taken when a sandblasted aluminum cathode was used, while those on the right were taken when a graphite coated (sandblasted) cathode was used. There was a noticeable density difference, with the plasma on aluminum cathodes being about a factor of two less dense than those on graphite coated cathodes.

The late time characteristics of material in the diode gap are relevant to repetitively pulsed diodes.<sup>11</sup> Interferograms taken at late times for a 3mm wide, graphite coated cathode are shown in Fig. 10. Once again, the direction of fringe shift indicates that the material consists mainly of neutrals. It can be seen that 50-100 $\mu$ s are required for the gap to clear, which is in agreement with results reported in Ref. 11. It was also found that the gap cleared out more quickly when the 3mm wide cathode was used than when the 25mm wide cathode was used. This is probably due to geometrical factors; it would be more difficult for material to leave the larger (25mm wide  $\times$  3.5mm gap, and so more closely resembling a parallel plate) diode, than to leave the smaller (3mm wide  $\times$  2.1mm gap) diode.

The spectral lines observed so far are listed in Table 2. The carbon and hydrogen lines were observed when either aluminum

or graphite coated cathodes were used. Aluminum lines were also observed when aluminum cathodes were used. No strong silicon or oxygen lines have been seen so far with either cathode. The intensities of the strongest CII(4267) and CIII(2296) lines were observed to be about a factor of six greater when carbon coated rather than aluminum cathodes were used. This factor of six was observed at both the 3 and 14kA/cm<sup>2</sup> current densities. The H $\alpha$  line intensity was similar for both aluminum and graphite coated cathodes. The ratio of the CIII line intensity to that of the CII line was higher at higher current densities, as would be expected.

For a plasma in local thermodynamic equilibrium, the line intensity ratio is given by<sup>7</sup>

$$\frac{I(\text{CIII})}{I(\text{CII})} n_e \propto T_e^{3/2} e^{-\Delta E/T}$$

where  $\Delta E$  is the energy difference between upper levels of the two transitions and the proportionality constant depends on the atomic parameters. The plasma densities measured here are far too low for LTE to be established on this timescale. However, a rough temperature estimate may be obtained by assuming that the plasma equilibrates at some high density layer,

$$n_e = N_{eq}$$

very close to the cathode surface (closer than the 100 $\mu$  resolution of the interferometer), and that ionization states are frozen out, level populations are frozen out, and heating is negligible from that point on. Using the observed values of  $I(\text{CIII})/I(\text{CII})$  and choosing  $N_{eq} = 10^{19} \text{cm}^{-3}$ , (for which equilibrium is established in about 1ns<sup>7</sup>) yields  $T_e$  estimates of 2.9(3.2)eV for the 3(14)kA/cm<sup>2</sup> cathode. While this model is admittedly quite crude and sensitive to

the rather arbitrary choice of  $N_{eq}$ , a change in the product  $I(CIII)/I(CII) \times N_{eq}$  of a factor of ten will change the inferred temperature by only  $\sim \pm 0.5\text{eV}$ . A more accurate characterization, using the time dependent collisional-radiative model,<sup>1,2</sup> will be carried out in the future. All of this is predicated on the assumption that the plasma is optically thin; this was checked by placing a spherical mirror behind the plasma so that light incident on the mirror was reflected back through the plasma to the monochromator entrance slit. This would theoretically double the signal for an optically thin plasma, although losses in the optics will limit this somewhat. The CIII and CII intensities showed close to a factor of two increase when the mirror was used, so the assumption of an optically thin plasma seems reasonable.

When aluminum cathodes were used, the aluminum line emission did not show a vastly different time dependence than that of the carbon line emission. In Fig. 11, the intensities of AlIII and CIII lines are shown for an aluminum cathode shot. This would imply that surface contaminants, here indicated by the carbon, enter the plasma on a similar timescale as the cathode substrate material.

Aluminum cathodes were coated with a thin layer of silicone diffusion pump oil to see what effect this had on silicon line emission. The coating was thin on a macroscopic scale but quite thick on a microscopic scale. In Fig. 12, the intensities of the SiII line at  $4130\text{\AA}$  are compared for cathodes with and without an oil coating. The line intensity was almost lost in the continuum background when an uncoated cathode was used and was noticeably enhanced when the cathode was coated with oil.

The cathode plasma expansion velocity was not measured directly; however, it was inferred from the impedance time history to be about 2cm/ $\mu$ s. It is important to note that this inferred velocity was similar for both aluminum and graphite coated cathodes and similar for all current densities.

### Discussion

The plasma density difference between aluminum and graphite coated cathodes, the increase in carbon line emission when graphite coated cathodes were used and the increase in silicon line emission with a silicon oil coating all show that the cathode plasma is affected by the choice of cathode material and/or surface condition. On the other hand, the observed hydrogen lines (and carbon lines with aluminum cathodes) clearly show that the cathode plasma is at least partly composed of materials from surface contaminants.

Since the inferred cathode plasma expansion velocity was similar for both cathode materials, it would seem that cathode plasma expansion is caused by impurity materials, most probably hydrogen due to its lower mass. The inferred expansion velocities are consistent with the 3eV temperature estimates if the expansion is due to protons, and the fact that the expansion velocity seemed to change little with changing current density is consistent with the fact that temperature estimates also changed little with current density.

The fact that both substrate and impurity materials are observed suggest that there may be a competition between the two to

determine the makeup of the cathode plasma, since there is more than enough material in a few monolayers of oil to account for the entire plasma inventory. This is consistent with the similar observed time dependences of substrate and impurity line emission, and with the fact that a macroscopic increase in silicone oil coating caused an increase in silicone line emission. While the cathode plasma will be affected somewhat by the choice of cathode material and surface condition, it seems that the impurity components (i.e. protons) must be removed from the plasma to reduce the expansion velocity. To eliminate these thin coatings in a practical vacuum system will be difficult indeed. If the plasma supply involves such a competition, however, it may be possible to effect a near removal of impurities from the cathode plasma with cleaning procedures that remove most, but not all, of any impurities from the cathode surface. Since the plasma required to short the gap is usually a small percentage of the total plasma inventory ( $\leq 3\%$  in this experiment), the requirements on plasma purity will be fairly strict.

If the number of emission sites is proportional to the total current (with each site carrying a fixed current) and most of the plasma heating occurs near the emission sites, then the temperature would be independent of current density and the plasma density would be linearly proportional to the current density. The results of this experiment are not inconsistent with such a picture. This is analogous to the case of vacuum arcs, where the number of cathode spots has been observed to be proportional to the total arc current.<sup>13</sup>



In conclusion, the cathode plasma density increases with increasing current density, the plasma inventory increases with time and the material in the cathode-anode gap becomes neutral-dominated soon after the pulse. While some properties of the cathode plasma depend on the cathode material and surface condition, the plasma expansion is caused by protons from residual surface contaminants.

### References

1. P.F. Ottinger, Shyke A. Goldstein, J. Guillory, and V.K. Tripathi, "Cathode plasma filamentation in pinch-reflex diodes", Bull. Am. Phys. Soc. 27(8, II), 1121, Oct. 1982.
2. A.S. Toepfer and L.P. Bradley, "Plasma instabilities in high current field emission diodes", J. Appl. Phys. 43(7), 3033-3036, July, 1972.
3. A. Palevsky, G. Bekefi, and A.T. Drobot, "Numerical simulation of oscillating magnetrons", J. Appl. Phys. 52(8), 4938-4941, Aug. 1981.
4. C.M. Gilman, P.S. Sincerny, R. Stringfield, G.I. James, and B.D. Harteneck, "Radiation driven surface ablation", IEEE Cat. 82CH1770-7, 72 (1982).
5. D.D. Hinshelwood, "The effects of current flow on cathode plasma formation in REB diodes", IEEE Cat. 82CH1770-7, 138 (1982).
6. Acheson Colloids, Port Huron, Mi.
7. H.R. Griem, Plasma Spectroscopy, McGraw-Hill, New York 1964, Ch. 6.
8. Chemical Rubber Company, Handbook of Chemistry and Physics, 48th ed, p. E-159 (1967).
9. G.P. Bazhenov, E.A. Litvinov, G.A. Mesyats, D.I. Proskurovskii, A.F. Shubin and E.B. Yankelevich, "Supply of metal to the cathode burst in explosive electron emission from metal tips", Sov. Phys. Tech. Phys., 18(6), 795-802, Dec. 1973.
10. Shyke A. Goldstein, Jaycor (private communication)
11. B. Fell, R.J. Comisso, V.E. Scherrer, and I.M. Vitkovitsky, "Repetitive operation of an inductive driven electron-beam diode", NRL Memo report 4714, January 1982.

12. R.W.P. McWhirter in Plasma Diagnostic Techniques, ed. by Huddleston and Leonard, Academic Press, New York 1965, Ch. 5.
13. L.P. Harris in Vacuum Arcs, ed by Lafferty, Wiley-Interscience, New York, 1980, Ch. 4.

Table I. Inferred Uniformity.

Uniformity

1. Sandblasted aluminum.
2. Graphite over sandblasted aluminum.
3. Graphite over smooth aluminum.
4. Smooth aluminum

Table II. Spectral lines observed

---

CI	2478 Å
CII	4267, 3918-20, 6579, 2836-37
CIII	2297, 4647-51
CIV	5801, 5811
H	6563 (H $\alpha$ ), 4861 (H $\beta$ )

The above lines were observed when either aluminum or carbon coated cathodes were used.

When aluminum cathodes were used, the following lines were also seen:

AlI 3962, 3944  
AlII 2815, 4663  
AlIII 4529

No oxygen lines have been observed with either cathode.

No strong silicon lines have been observed with either cathode.

---

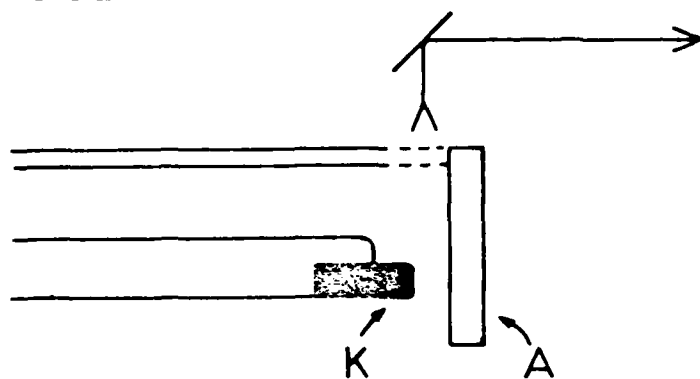
Figure Captions

- Fig. 1. Typical cathodes.
- Fig. 2. Experimental arrangement.
- Fig. 3. X-ray pinhole photograph and anode damage pattern showing relative uniformity.
- Fig. 4. (a) Typical waveforms  
(b) Interferograms; times indicated in 4(a).  
(c) Area viewed by the interferometer.
- Fig. 5. Interferogram showing neutral induced fringe shifts.
- Fig. 6. Current traces (a) and interferograms (b), (c) for three (peak) current densities.
- Fig. 7. Possible enhancement of current density from the top of the cathode due to incomplete magnetic diffusion.
- Fig. 8. Current traces (a) and interferograms (b) showing the effects of a pulse crowbar.
- Fig. 9. Current traces (a) and interferograms (b) for two different cathode materials.
- Fig. 10. Interferograms taken at late times.
- Fig. 11. Time dependence of carbon and aluminum line intensities.
- Fig. 12. Effect of a silicone oil coating.



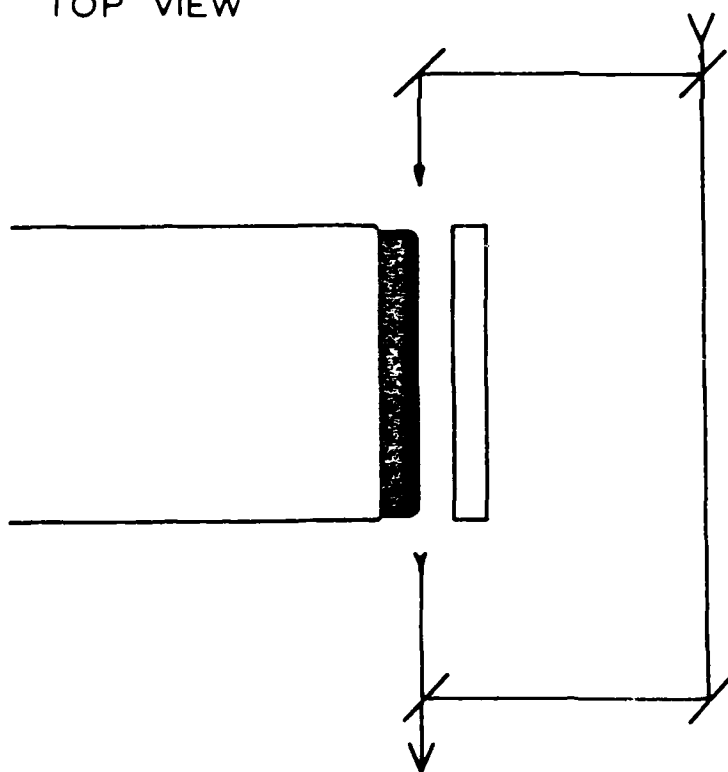
Fig. 1  
Hinshelwood

SIDE VIEW



.1 M MONOCHROMATOR  
.3 M MONOCHROMATOR  
.5 M SPECTROGRAPH

TOP VIEW



NITROGEN  
LASER  
INTERFEROMETER

Fig. 2  
Hinshelwood

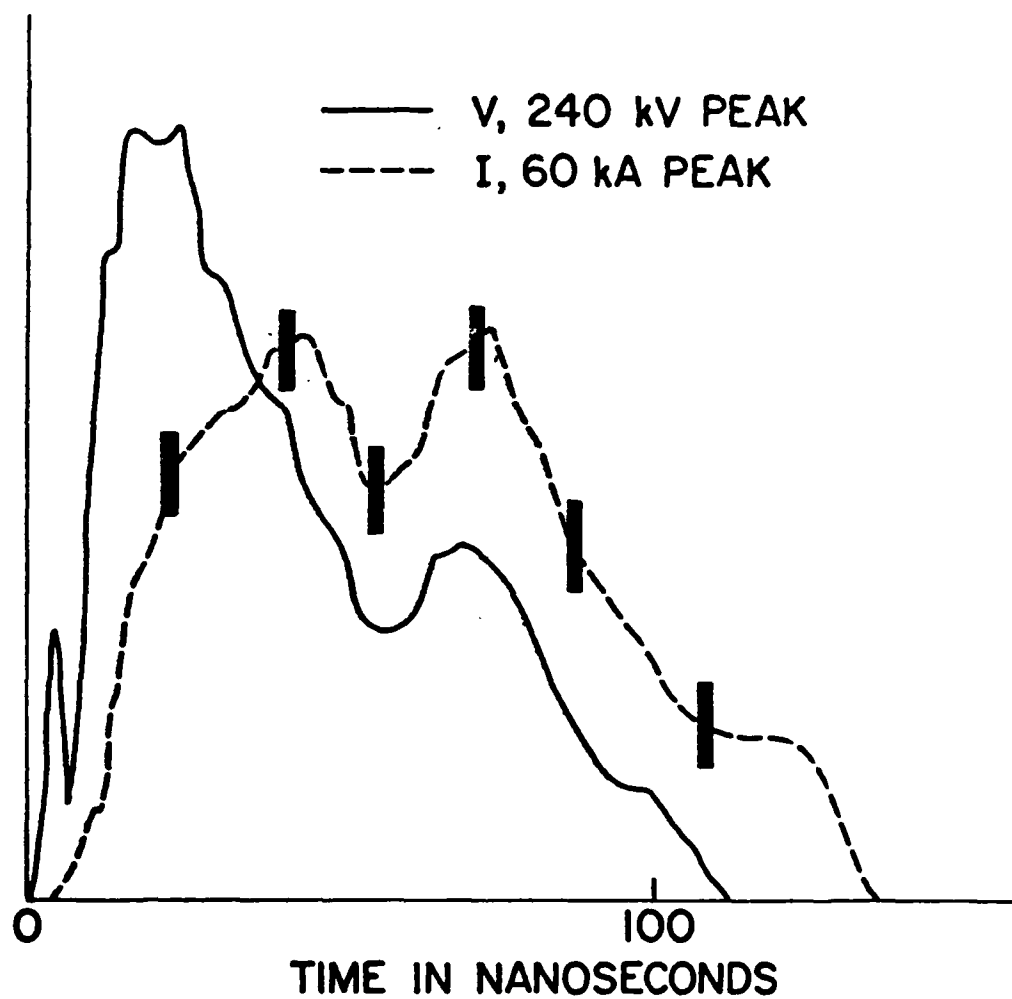


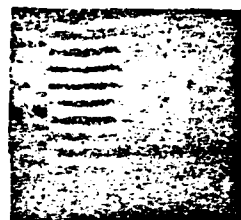
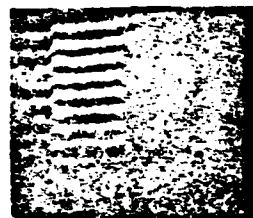
Fig. 3  
Hinshelwood



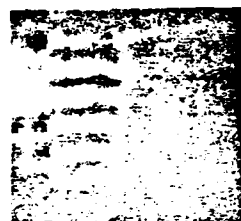
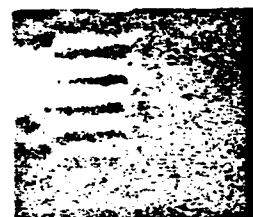
# REFERENCE

# SHOT

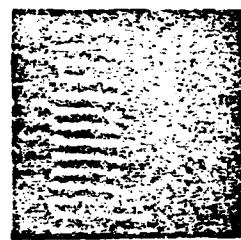
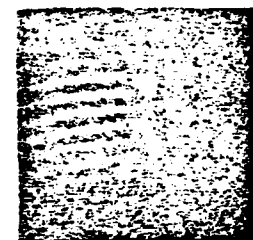
1



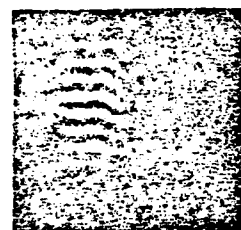
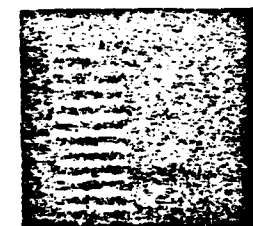
2



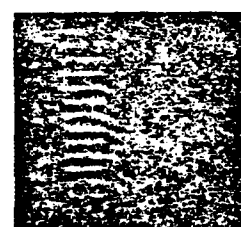
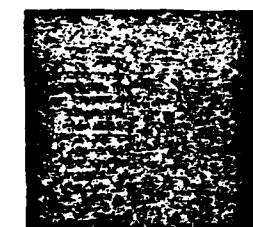
3



4



5



6

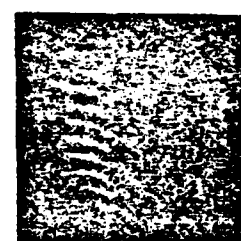
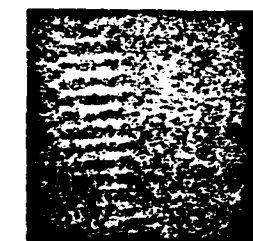


Fig. 4  
Hinshelwood

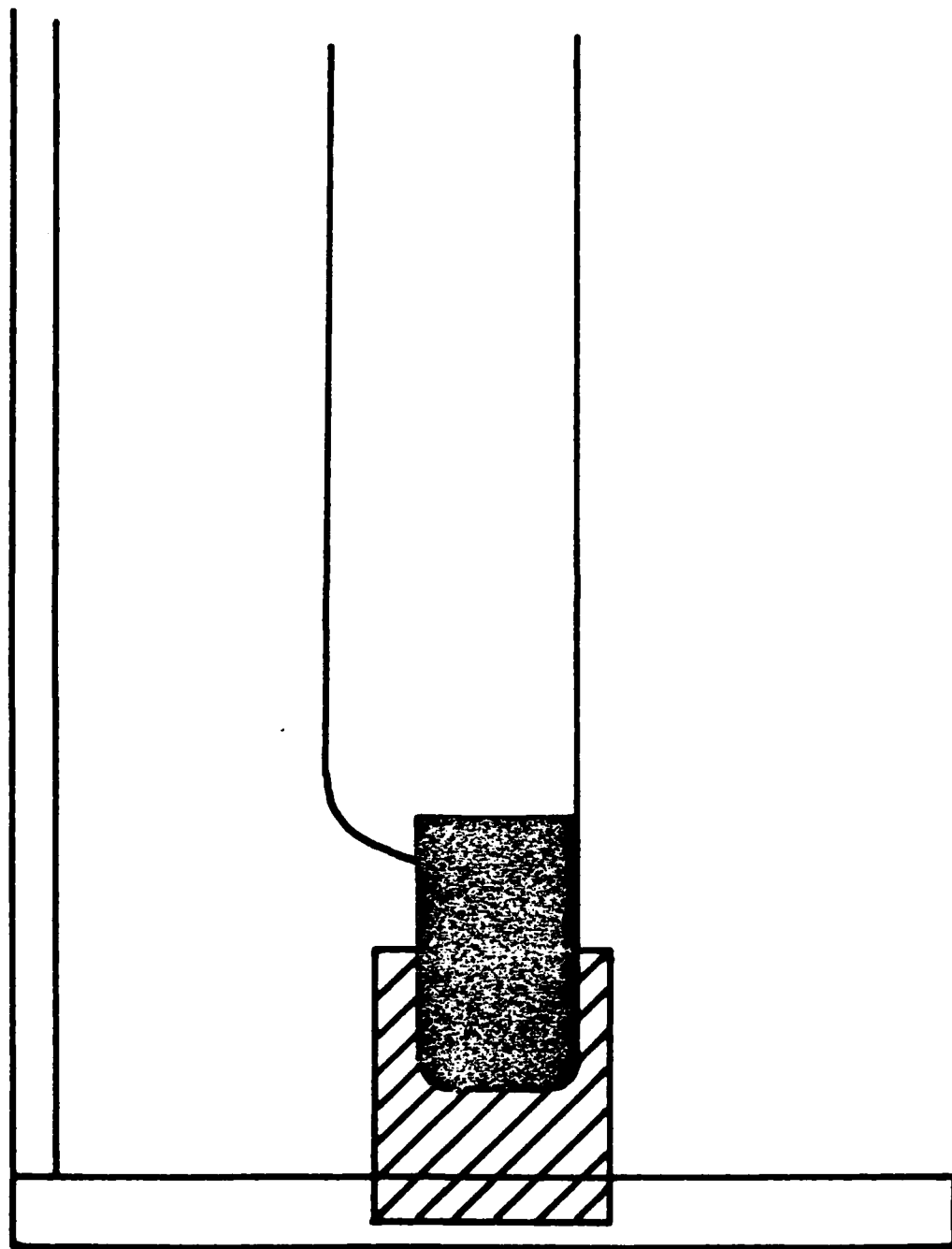


Fig. 5  
Hinshelwood



Fig. 6  
Hinshelwood

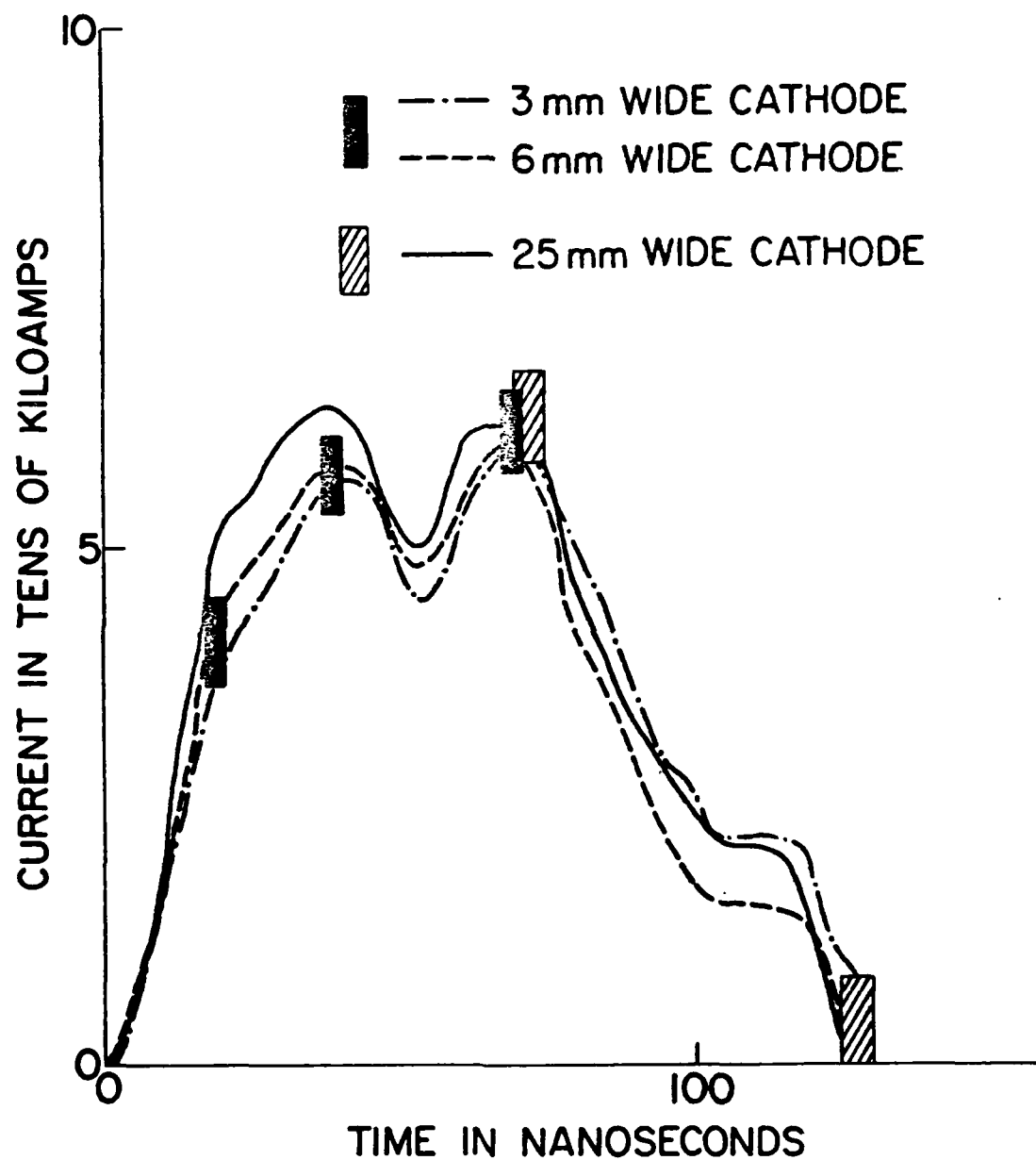
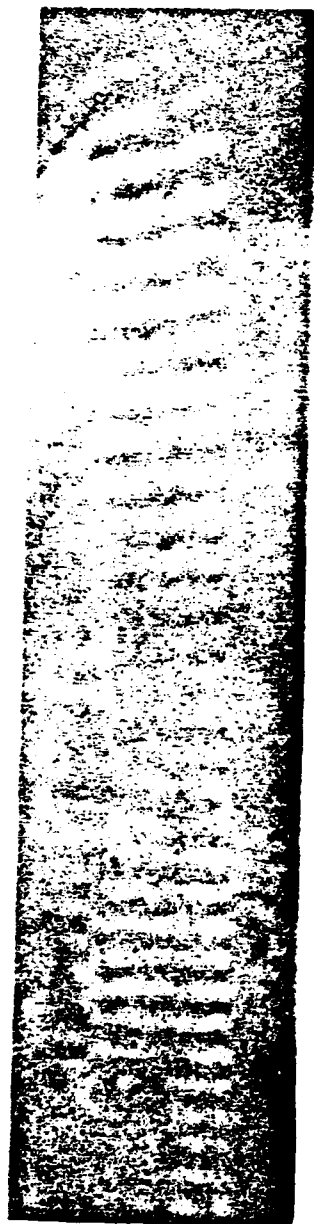


Fig. 7  
Hinshelwood

1



2

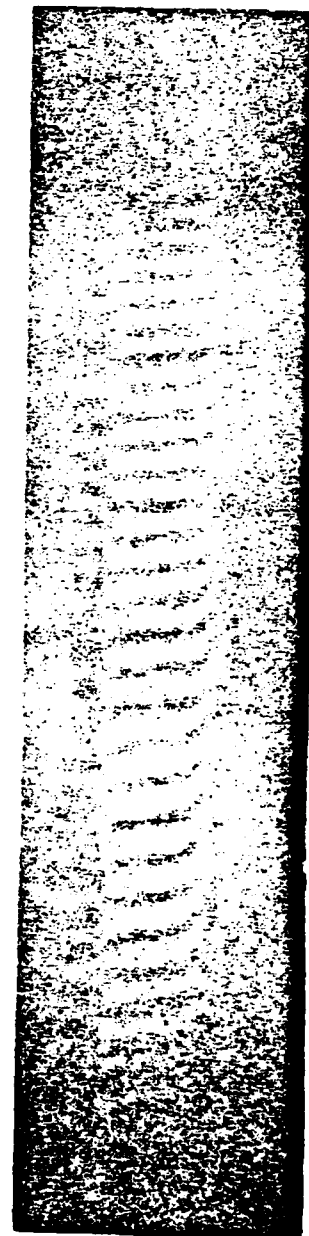
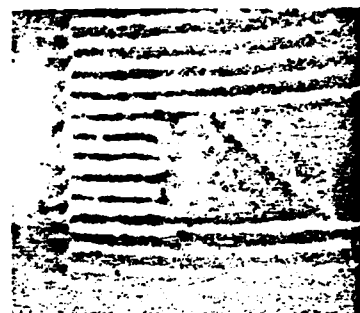
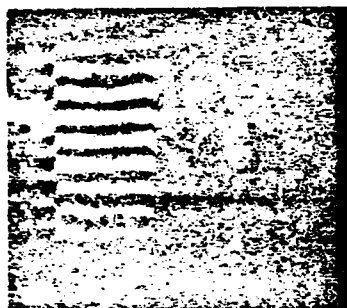


Fig. 8  
Hinshelwood

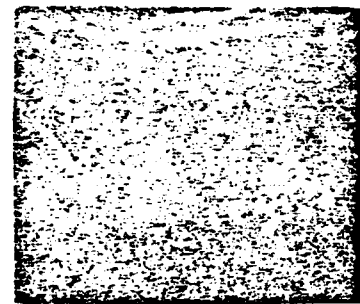
14 kA/cm<sup>2</sup>

27 kA/cm<sup>2</sup>

1



2



3

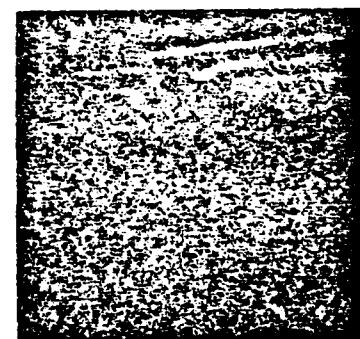
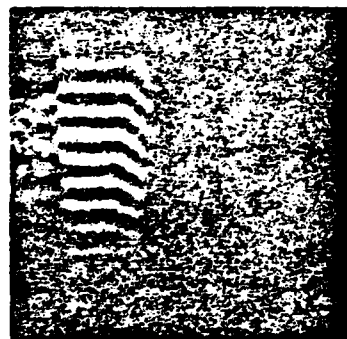


Fig. 9  
Hinshelwood

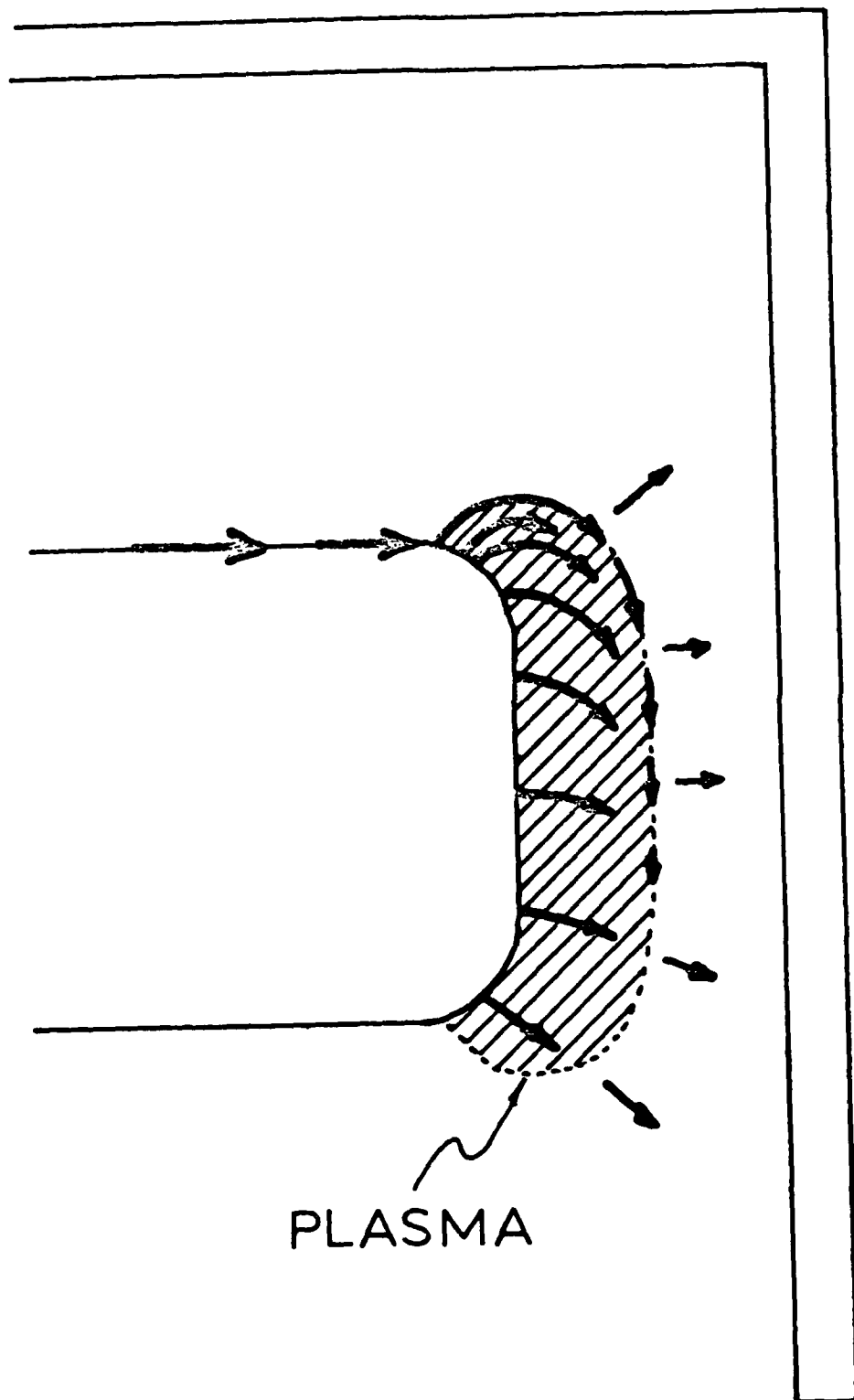


Fig. 10  
Hinshelwood

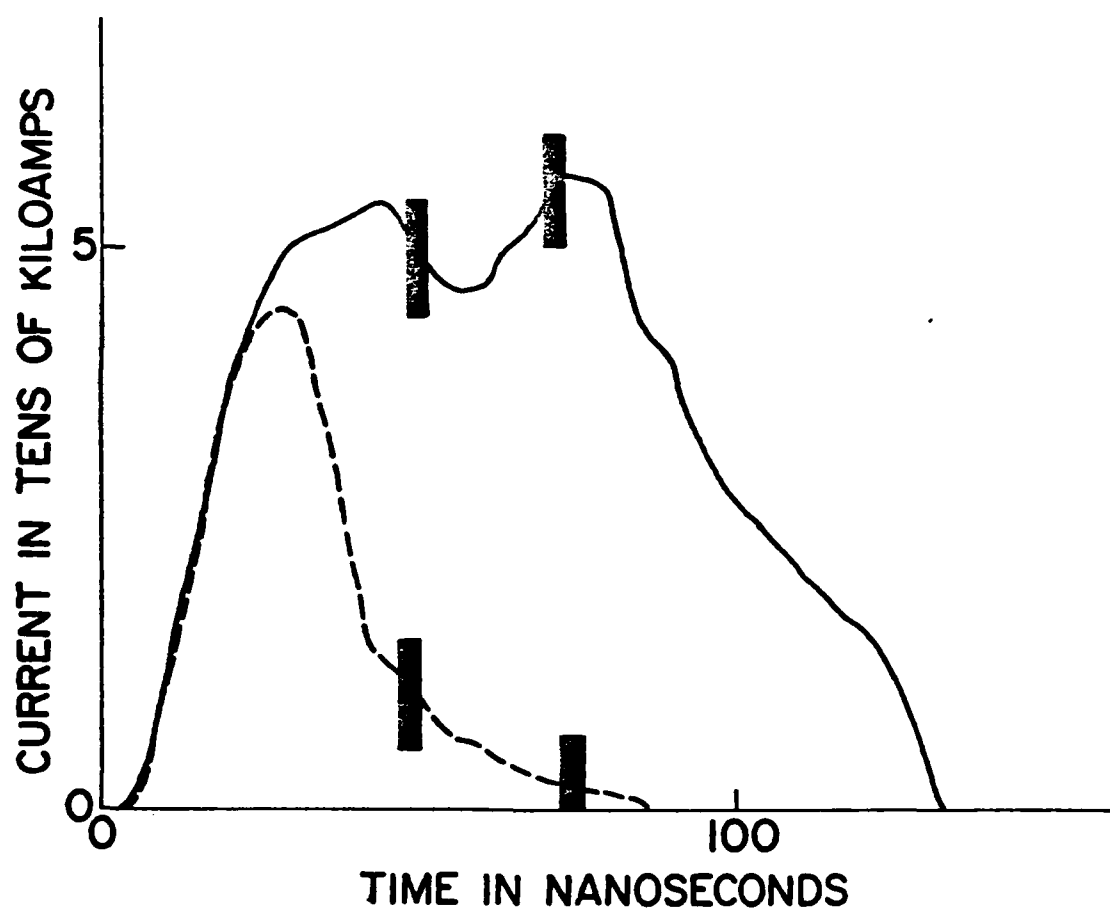


Fig. 11  
Hinshelwood



CROWBAR

FULL PULSE

1



2

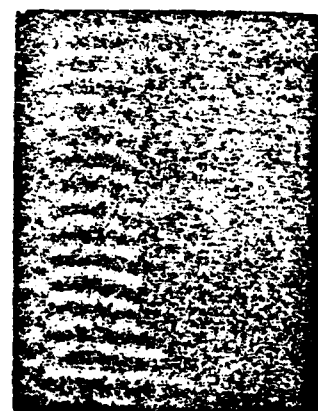
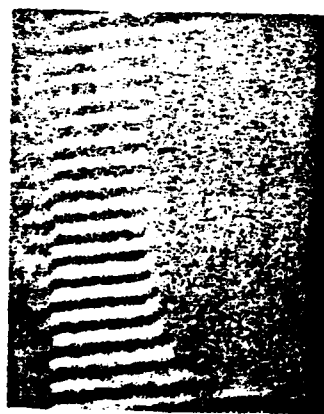


Fig. 12  
Hinshelwood

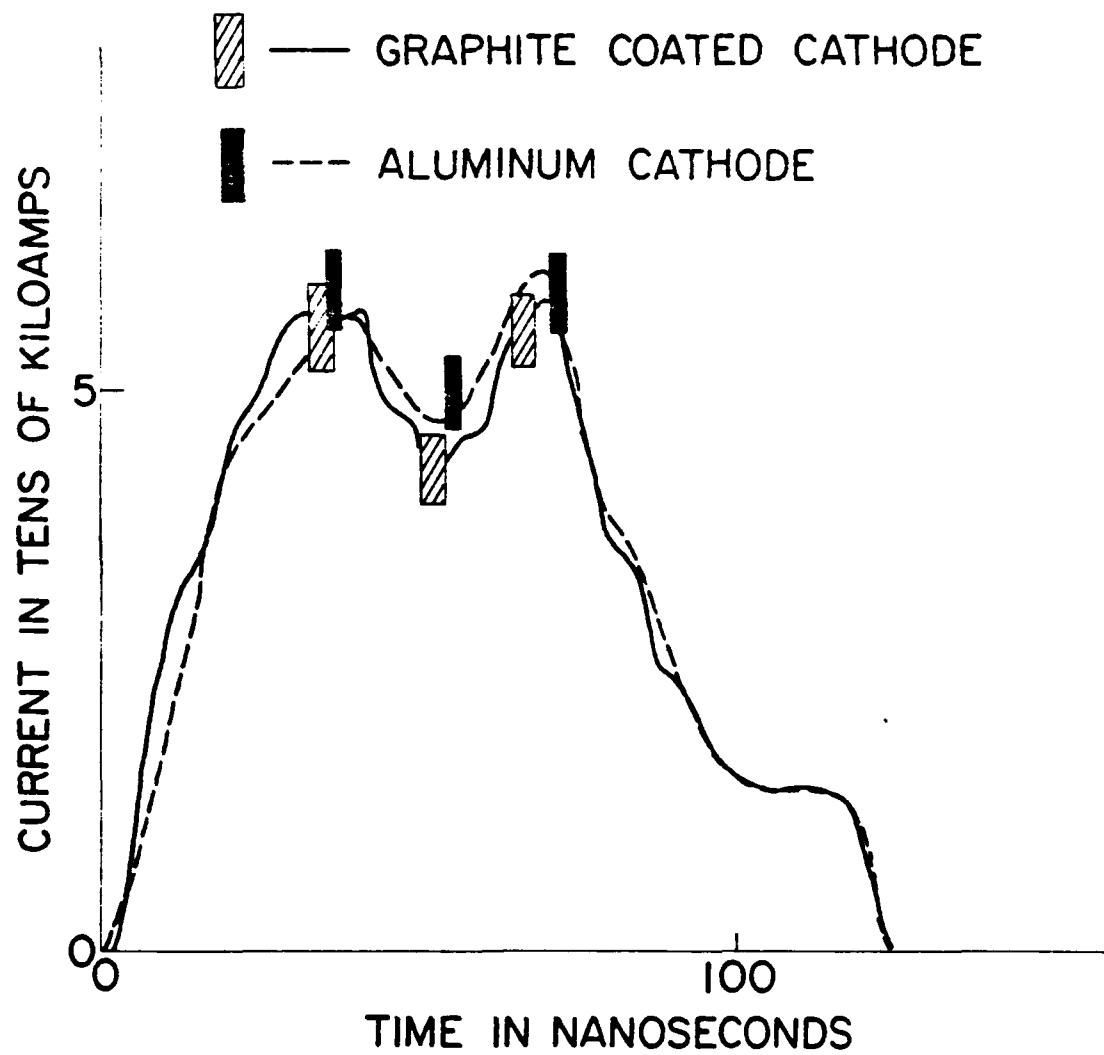
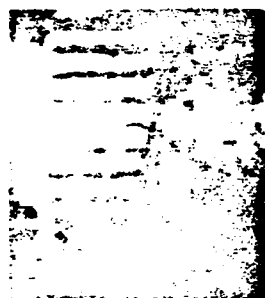


Fig. 13  
Hinshelwood

## ALUMINUM

1



2



3



## GRAPHITE

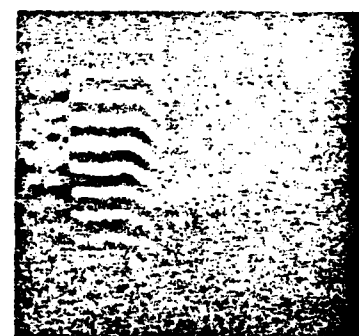
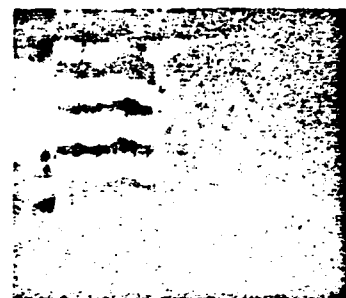
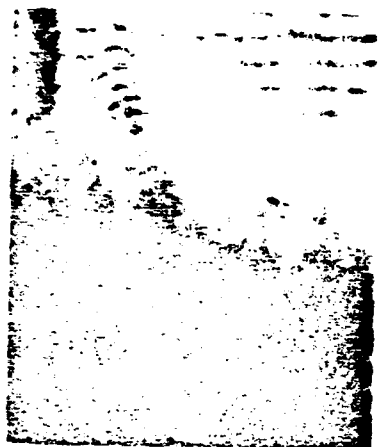
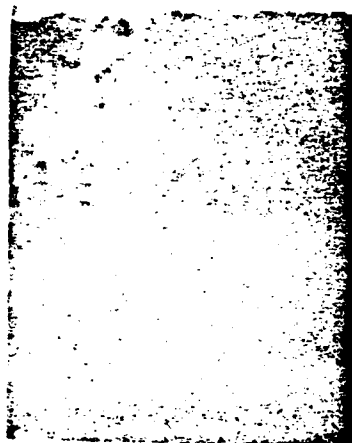


Fig. 14  
Hinshelwood



1  $\mu s$



10  $\mu s$



50  $\mu s$



100  $\mu s$

Fig. 15  
Hinshelwood

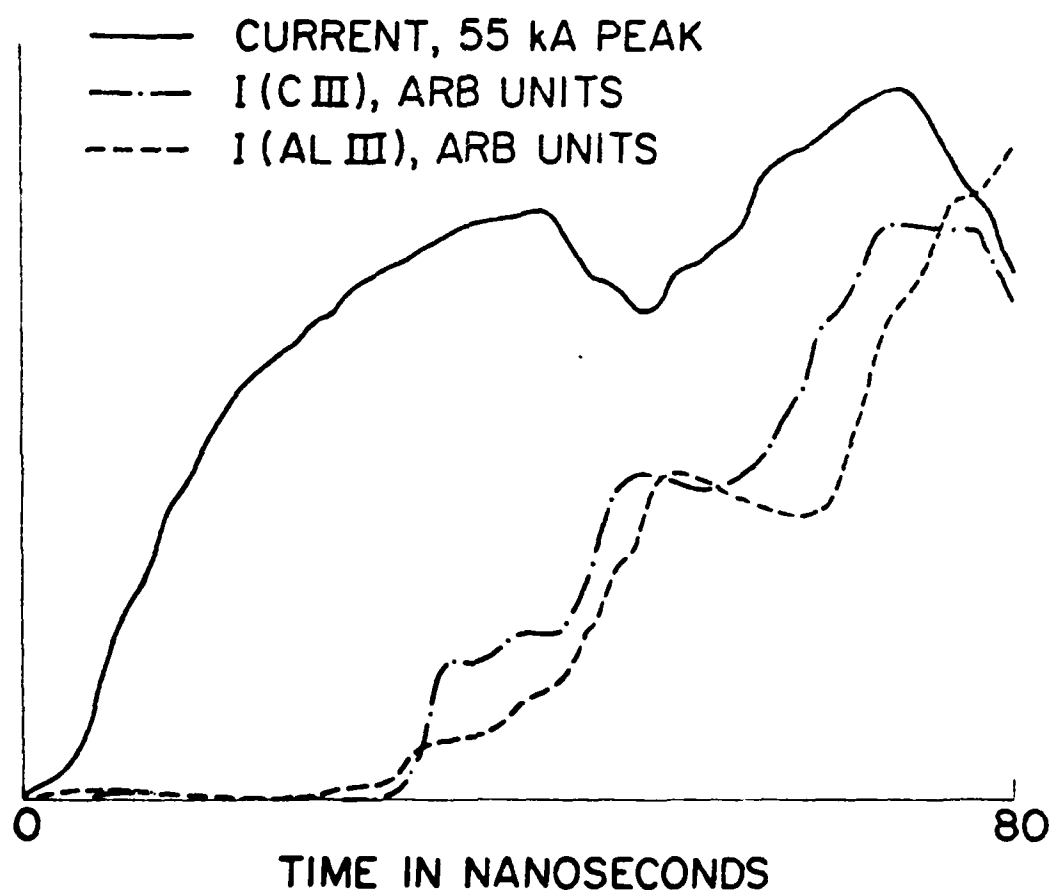


Fig. 16  
Hinshelwood

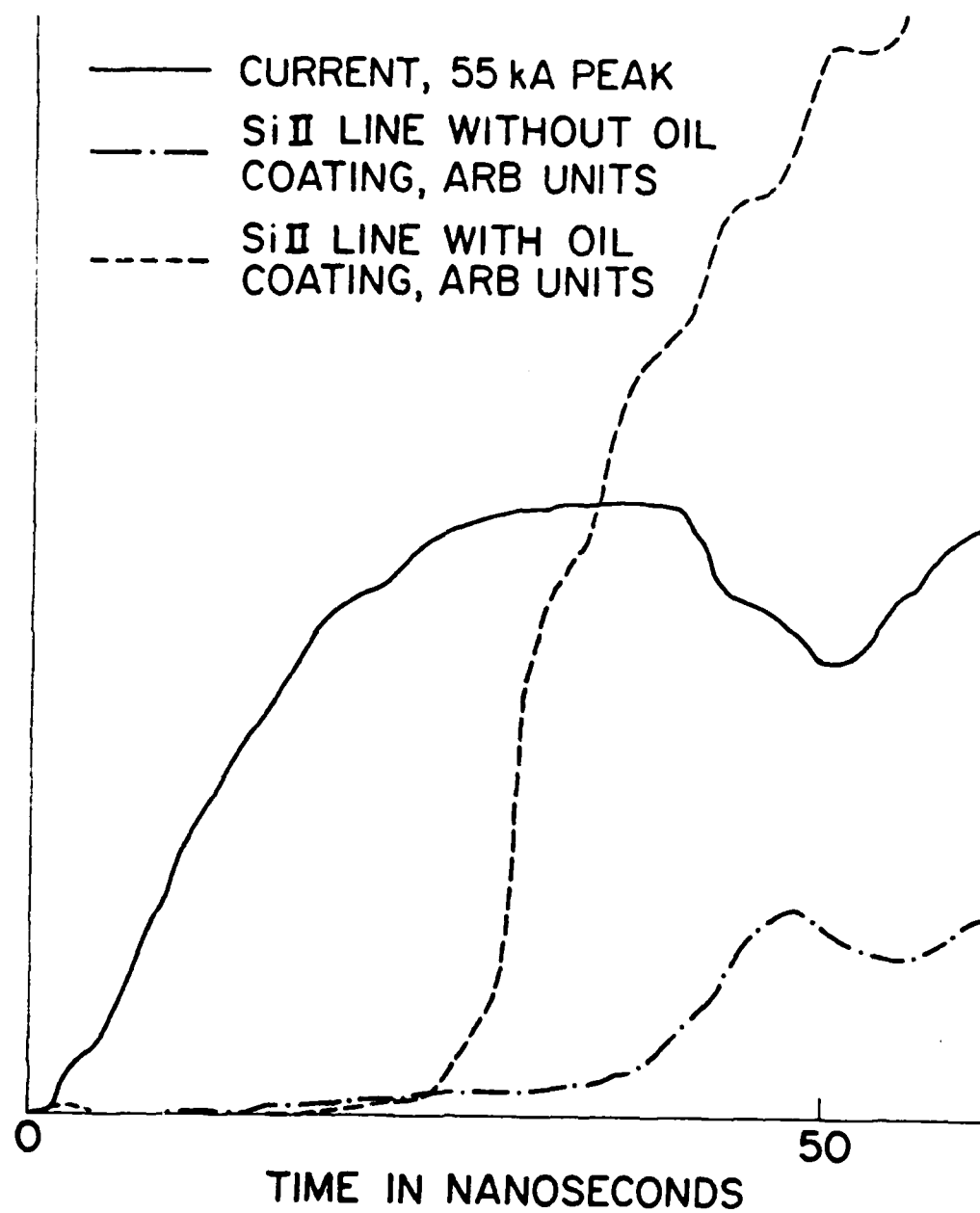
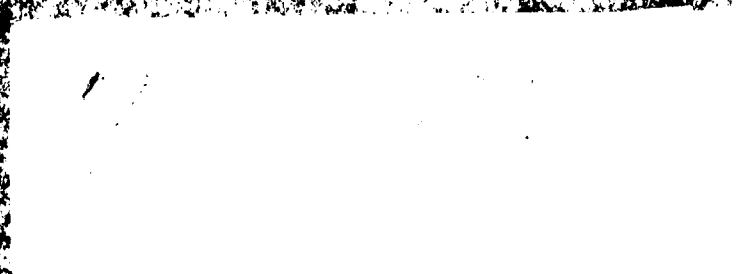


Fig. 17  
Hinshelwood

END

FILMED



DTIC